

A DUAL REFLECTOR FEED SYSTEM FOR A SUB-MM HOLOGRAM CATR

Janne Häkli, Tomi Koskinen, Juha Ala-Laurinaho, Jussi Säily, Anne Lönnqvist,
Juha Mallat, Jussi Tuovinen*, Antti V. Räsänen

MilliLab, Radio Laboratory, Helsinki University of Technology

*MilliLab, VTT Information Technology

email: janne.hakli@hut.fi

ABSTRACT – Manufacturing of large holograms for compact antenna test ranges can be facilitated with a modified hologram illumination. The relative quiet-zone size of the CATR can also be increased, which allows testing of larger telescope antennas with a fixed-sized hologram. The modified hologram illumination can be realized with a dual reflector feed system. In this paper, a simple ray tracing based synthesis technique for designing the dual shaped hyperbolic reflector feed system is described. Simulation results of a design example at 310 GHz are presented. The required accuracies in the reflector system assembly are also discussed.

INTRODUCTION

Several satellites carrying scientific instruments and antennas at sub-mm wavelengths (frequencies above 300 GHz) are scheduled for launch during this decade. The electrical testing of these telescopes is very demanding or even impossible with existing antenna measurement facilities. Conventional far-field antenna measurements are not applicable for large sub-mm wave antennas due to the required long far-field distance and the high atmospheric attenuations – the very reason for space-borne instruments. Near-field measurements are one option, but the measurements are very time consuming, as the required number of field samples is very large for accurate computation of the antenna radiation pattern. The compact antenna test range (CATR) is seen to be potentially the best antenna testing method at sub-mm wave frequencies [1].

In a compact antenna test range a collimating element forms the planar wave needed for antenna testing from a spherical wave radiated by a feed. The region, where the planar wave exists, is called the quiet-zone (QZ) of the CATR. Typically, the QZ is allowed to have at maximum 1 dB peak-to-peak ripple in amplitude and 10° in phase.

A set of reflectors, usually two reflectors, is commonly used as a collimating element in CATRs at microwave and millimeter wave frequencies up to 200 GHz. A binarized computer-generated amplitude hologram can also be used as a collimating element for a CATR [2]. The hologram pattern is manufactured by etching slots onto a copper-plated Mylar film. The hologram is a transmission type planar structure with inherently lower surface accuracy requirements than the requirements for reflectors. The hologram is tensioned into a frame to ensure sufficient surface flatness. The realization of a CATR based on a hologram is significantly more economical at sub-mm wave frequencies than the corresponding CATR based on reflectors, because the hologram manufacturing is less costly than manufacturing of large accurate reflector surfaces and only one hologram is needed for the CATR. An additional advantage is that the hologram is

lightweight, which allows the disassembly and transportation of the CATR to a different location. The basic structure of the hologram-based CATR is illustrated in Figure 1 with an example of the hologram pattern. Absorbers are placed around the CATR to reduce disturbances from the reflections from surrounding structures.

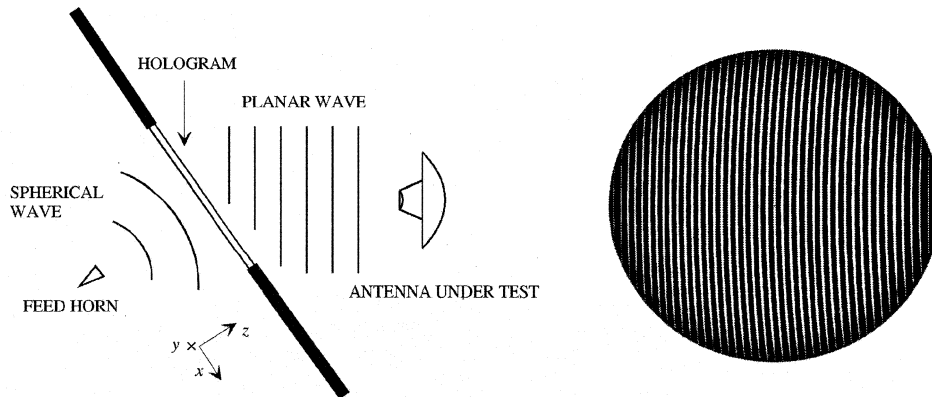


Figure 1. CATR based on hologram and an example of the hologram pattern

Testing of a large telescope requires a larger hologram than the telescope antenna aperture. The manufacturing of large sub-mm frequency holograms is the main challenge in the realization of a large hologram-based CATR. The large hologram patterns have to be combined from several separately etched hologram pieces that are soldered together as hologram patterns cannot be currently etched on larger films than 1.5 meters by 6.0 meters. These seams cause disturbances to the QZ field. The slots in the hologram pattern are narrowed towards the hologram edges to realize an amplitude taper to the hologram aperture, which reduces edge diffraction disturbances to the desired plane wave. Etching of narrow slots (below 100 μm) is difficult for large surfaces.

The work described in this paper aims to decrease the size of the hologram needed for testing a telescope in a CATR with an improved feed system. In addition, the hologram fabrication is simplified by widening the narrow slots at the hologram pattern edges. These benefits can be achieved by introducing an amplitude taper with controlled phase into the hologram illumination. The improved illumination can be realized with a dual reflector feed system (DRFS). A DRFS design example for a 600 mm hologram operating at the frequency of 310 GHz is presented.

MODIFIED HOLOGRAM ILLUMINATION

Hologram manufacturing can be facilitated by modifying the hologram illumination to have an amplitude taper at the hologram edges. The amplitude taper reduces the need for narrowing the slots in the hologram pattern at the hologram edges. The resulting wider slots are easier to etch. One example of suitable incident amplitude in the hologram aperture is a rotationally symmetric Butterworth-type amplitude distribution function

$$E(\rho) = \frac{1}{\sqrt{1 + \kappa \left(\frac{\rho}{\rho_0} \right)^{2N}}}, \quad (1)$$

where N is the order of the function, ρ is the radial distance from the hologram center and ρ_0 is the radial distance of the edge of the nearly flat part of function. The amplitude at this edge is determined with the parameter κ . The achievable relative quiet-zone size can be increased with the modified illumination. This allows testing of larger telescopes with a fixed-sized hologram. Holograms were designed for two test cases: for a large quiet-zone size and for more constant slot widths in the hologram pattern. The simulated quiet-zone for a 600 mm hologram at 310 GHz is shown together with the slots widths in the hologram pattern in Figures 2 and 3. In case 1 (Figure 2), the hologram was optimized for a large quiet-zone size. The illumination function used was (1) with $N=3$, $\rho_0=300$ mm and $\kappa=4.01$. The quiet-zone width is increased by 40 % and the narrowest slots are widened from 37.5 μm to 65 μm . In case 2, the hologram slot widths were chosen to be nearly constant over the hologram pattern, which facilitates the etching of the hologram pattern. The simulated QZ field amplitude together with the hologram pattern slot widths is shown in Figure 3. The illumination function (1) was chosen to have $N=5$, $\rho_0=210$ mm and $\kappa=1$. The slots in the pattern are 280–405 μm wide with the modified illumination.

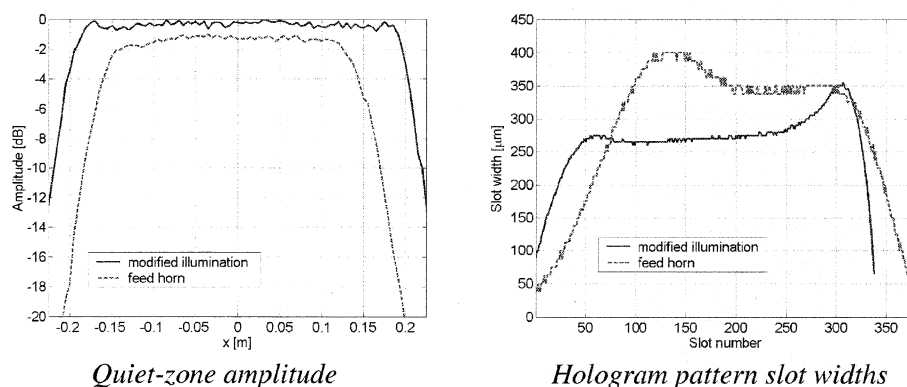


Figure 2. Case 1: simulation results for a hologram optimized for large quiet-zone size compared to a hologram illuminated directly by the feed horn.

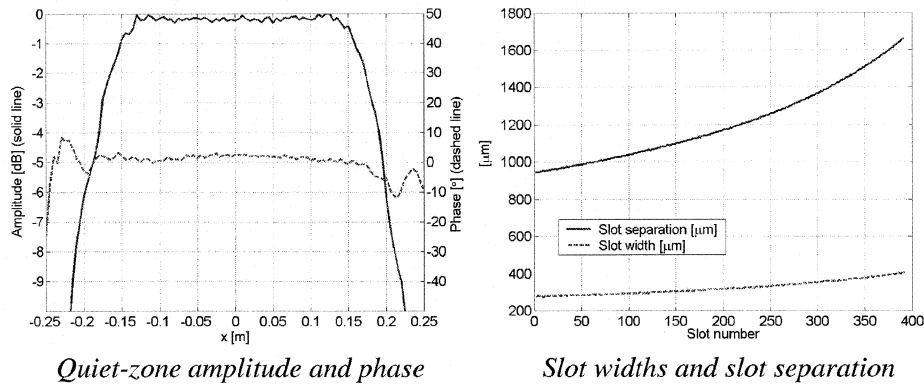


Figure 3. Case 2: simulation results for a hologram with nearly constant slot widths.

SYNTHESIS OF A DUAL REFLECTOR FEED SYSTEM FOR THE CATR

Dual reflector feed system (DRFS) can be used to modify the hologram illumination. Two reflecting surfaces are needed to control both the illumination amplitude and phase. The hologram illumination is a shaped beam. The DRFS beam has an amplitude of a Butterworth-function (1) in the hologram aperture with the phase of a spherical wave originating from the hologram focus. The DRFS was chosen to have a dual shaped hyperbolic geometry. The basic structure for a 600 mm hologram is shown in Figure 4. The hyperbolic reflector surfaces allow a compact structure together with a wide shaped beam needed for the hologram illumination. The first, the subreflector, has concave shape and the second, the main reflector, is convex. The reflectors are fed with a corrugated horn.

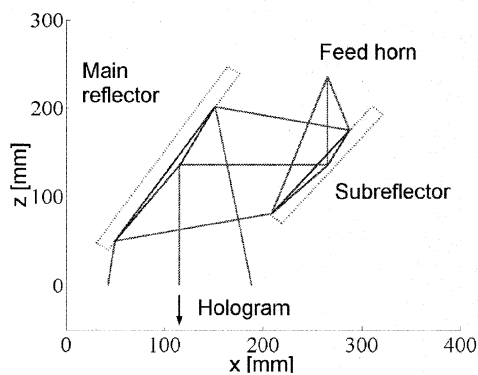


Figure 4. Schematic of the dual reflector feed system.

The subreflector center is located at the distance of 100 mm from the feed horn and the separation of the reflector centers is 150 mm. The design of the reflector surfaces is a dual shaped reflector synthesis problem. Shaped reflectors for shaped beam applications can be synthesized with several methods. Commercially available synthesis software are usually intended for satellite antenna applications with contoured beams. As the

hologram DRFS differs from the common applications, a simple specialized synthesis method was developed and implemented as MATLAB[®]-software. The used method is based on the method described in [3] with some modifications.

The synthesis of the hologram DRFS is based on ray-tracing, i.e., on geometrical optics (GO). The advantages of the GO method are that no initial surfaces are needed as in many diffraction synthesis methods and the method is straightforward and simple. The high frequency facilitates the use of a simple GO synthesis as the reflectors are relatively large in wavelengths. The main disadvantage of the method is that it does not take into account the diffraction effects. The GO synthesis is commonly used as the starting point for diffraction synthesis optimization in satellite communication antenna applications.

In geometrical optics, the electromagnetic fields are approximated with rays that propagate straight between the reflections. The rays in DRFS synthesis procedure were chosen to contain only the power density (amplitude) and phase information. The power is considered to propagate in flux tubes bounded by adjacent four rays. The ray path length determines the phase for each ray. The reflectors are assumed locally planar at the reflection points and the surface normal at each point is computed with reflection law (Snell's law) from the desired ray path.

The ray distribution in the hologram aperture, i.e., flux tubes, determine the illumination amplitude in the aperture. An even-angled ray distribution in spherical coordinates is used to describe the feed horn radiation. The ray distribution corresponding to the desired hologram illumination is solved in polar aperture coordinates from

$$P_{out} = P_{in} = \int_{\rho_1}^{\rho_2} \int_{\phi_1}^{\phi_2} \frac{E(\rho, \phi)^2}{C} \rho d\phi d\rho, \quad (2)$$

where $E(\rho, \phi)$ is the amplitude of the electric field and C includes all coordinate independent terms (for example the wave impedance). The electric field power density $E(\rho, \phi)^2$ is assumed to be piecewise linear in radial direction for easy solving of ρ_2 from (2) using the conservation of power within the flux tubes. The reflector surfaces are determined so that they transform the feed horn even-angled ray distribution into the ray distribution in the hologram aperture, which corresponds to the desired hologram illumination.

The synthesis procedure starts with the center ray path. This ray goes from the feed phase center to the sub-reflector center and reflects there to the main reflector center ending up at the hologram center. The center incident and reflected rays form 90° angles. The surface normal is then computed with reflection law from the incident and reflected rays. The surface tangent plane is easily determined from the normal vector for both reflector surfaces. The next ray is launched from the feed phase center towards the subreflector. The intersection point of this ray and the tangent plane is the next sub-reflector surface point. The new surface normal is calculated from the direction of reflected ray for the required ray path. The synthesis proceeds from the reflector centers towards the edges in counter-clockwise direction. Previously computed surface normal

at the closest known point in radial direction towards the reflector center from the current point is used to determine the local tangent plane at the current point. The main reflector is determined similarly by launching rays from the hologram focus to the hologram aperture (reflected rays) and using the rays from the corresponding subreflector points as incident rays. Finally, the phase of hologram illumination is corrected to the phase of a spherical wave originating from the feed horn phase center by moving the main reflector surface point along the ray path from the hologram focus to the hologram aperture. Additional optimization of the phase may be done with phase correction obtained from the simulated phase performance of the DRFS.

DESIGN EXAMPLE

The synthesized reflector surfaces for a 600 mm hologram at 310 GHz are shown in Figures 5 and 6. The hologram illumination function used was (1) with $N=5$ and $\rho_0 = 210$ mm. Simulated quiet-zone field and hologram pattern slot widths are shown in Figure 3. The direction of the incident radiation is different in Figures 5 and 6 to better illustrate the reflector surfaces. The subreflector is concave, i.e., the feed horn is below the surface in Figure 4, and the main reflector is convex with the hologram and the subreflector above the surface in Figure 5. The dimensions of the shaped reflector surfaces are approximately $166 \text{ mm} \times 119 \text{ mm} \times 2.7 \text{ mm}$ and $122 \text{ mm} \times 83 \text{ mm} \times 4.6 \text{ mm}$ for the main reflector and the subreflector, respectively. The edges of the shaped reflector surfaces are rounded to reduce edge diffraction and flat plates were added to the reflector surfaces to allow simulation of the surfaces milled out of metal plates.

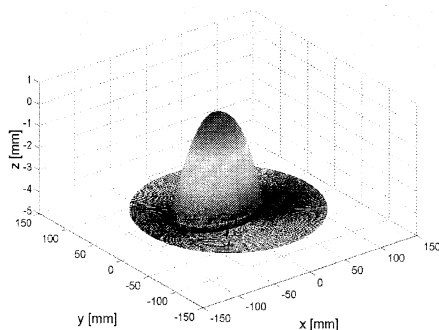


Figure 5. Subreflector surface (inverted).

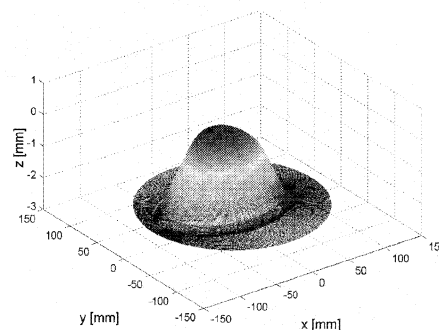


Figure 6. Main reflector surface.

The applicability of the GO synthesis method for the DRFS design was verified with simulations of the DRFS radiation. The simulations were done with commercial reflector antenna analysis software GRASP8W. Physical optics (PO) and physical theory of diffraction (PTD) were used to compute the DRFS radiation at the hologram aperture. The focal length of the hologram was 1.8 meters and the near-field radiation of the dual reflector feed system was computed at the corresponding distance from the DRFS. The simulated DRFS radiation is presented in Figures 7 and 8 for the horizontal amplitude cut and for the vertical amplitude cut of the hologram aperture field, respectively. The objective was the 5th-order Butterworth-illumination. The phase in the center crosscut of the aperture field compared to the desired ideal spherical wave is

shown in Figure 9. The simulated cross-polarized field at the hologram center is presented in Figure 10. Both of these aperture cuts are in the horizontal direction.

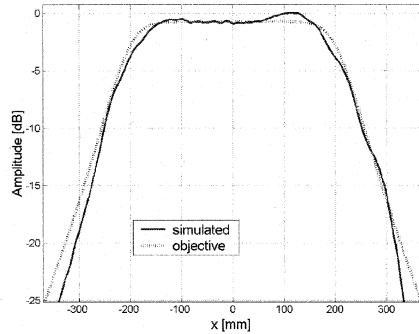


Figure 7. Amplitude in a horizontal cut.

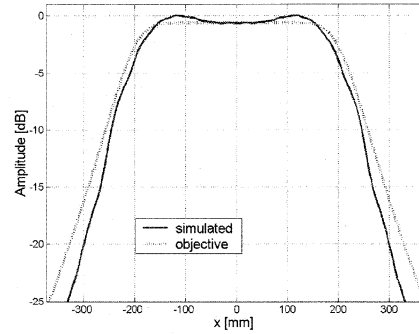


Figure 8. Amplitude in a vertical cut.

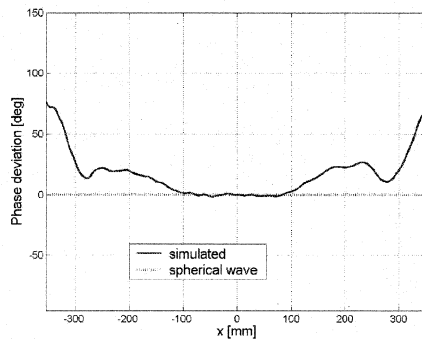
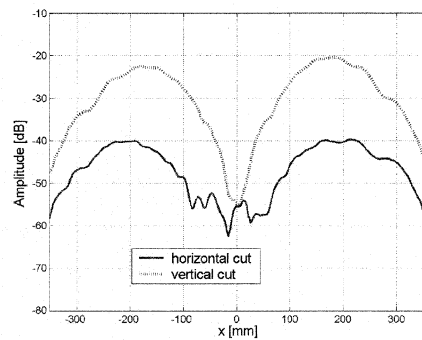


Figure 9. Simulated phase in a horizontal cut. Figure 10. Cross-polarization.



The deviation of the simulated DRFS performance from the desired Butterworth-type illumination is mainly due to edge diffraction. The edge diffraction could be reduced with further optimization of the DRFS structure and with using lower edge illumination both in the hologram illumination (edge taper on the main reflector) and in the feed horn beam (edge taper on the subreflector). The 310 GHz corrugated horn used has a wide beam, which makes the reflector sizes inconveniently large for lower than -15 dB edge taper on the subreflector.

Manufacturing and assembling of the dual reflector feed system

Phase and amplitude errors in the incident field on the hologram cause errors to the QZ field, which are roughly of the same order of magnitude as the errors in the incident field. Therefore, to satisfy the QZ field quality requirement of 1 dB amplitude and 10° phase ripple (peak-to-peak), the hologram illumination ripples are allowed to be at maximum half of these. The main DRFS manufacturing related causes for the hologram illumination deviations from the desired are the accuracy of reflector surface milling and the potential misalignment of the reflectors.

Assuming the RMS-surface error in the milling to be of the order of $2 \mu\text{m}$, the RSS-phase error caused by the two reflections in the reflector system can be estimated to be about 2° . If the phase errors caused by the misalignment of reflectors and the feed horn are independent of milling errors, the maximum allowed phase deviation due to the misalignments is about 4.5° for the total RSS-error of 5° in the hologram illumination. The total phase deviation caused by the misalignment can be estimated to be

$$\Delta\varphi_{\text{misalignment}} = \sqrt{\Delta\varphi_{\text{feed}}^2 + \Delta\varphi_{\text{sub}}^2 + \Delta\varphi_{\text{main}}^2}. \quad (3)$$

Assuming that the deviations caused by the feed horn ($\Delta\varphi_{\text{feed}}$), the subreflector ($\Delta\varphi_{\text{sub}}$) and the main reflector ($\Delta\varphi_{\text{main}}$) have an equal and independent contribution to the total phase deviation in the DRFS beam, the allowed phase deviation caused by each of them is approximately 2.6° . The effect of the reflector (or feed horn) dislocation and misalignment was studied with GRASP8W simulations. In the simulations, the other objects were kept at their correct locations and alignment, while the reflector (or horn) under investigation was moved or rotated. Simulation results for subreflector displacement in z -direction, i.e., when the subreflector distance from the feed is changed, are shown in Figures 11 and 12 in horizontal and vertical cuts at the center of the hologram aperture, respectively. The phase is compared to the beam of the perfectly aligned DRFS.

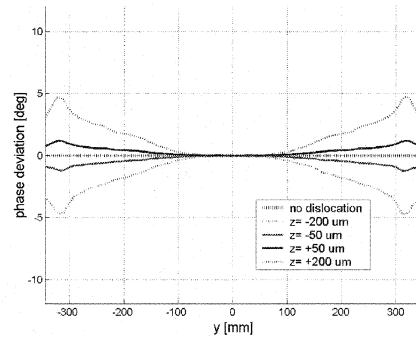
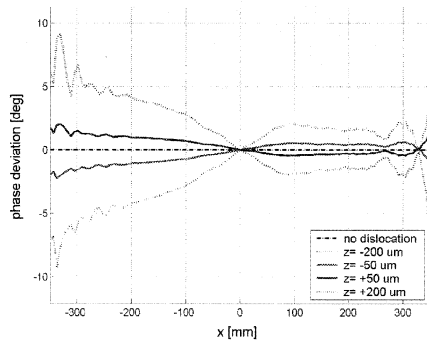


Figure 10. Phase deviation (horizontal cut). Figure 11. Phase deviation (vertical cut).

In the simulations with several examples of dislocations and misalignments, an approximately linear dependence between the amount of the misalignment and the resulting phase deviation was observed. The amplitude deviations were observed to correspond with the amount of the phase deviation in the simulation. The maximum allowed amplitude deviation could have been determined similarly to the phase deviations that were discussed here. The estimated location and alignment accuracies of the DRFS assembly are shown in Table 1. The rotation tolerance around the x -axis is estimated to be about the same as the tolerance of the y -axis rotation.

Table 1. Estimated accuracies required for the reflector (feed) locations and alignment.

	Dislocation in x-direction	Dislocation in y-direction	Dislocation in z-direction	rotation around the y-axis	rotation around the z-axis
Feed	<20 μm	<20 μm	<100 μm	<0.007°	<30°
Subreflector	<20 μm	<20 μm	<100 μm	~0.005°	~0.12°
Main reflector	<20 μm	<20 μm	<100 μm	<0.007°	<0.2°

The required accuracies for the reflector locations and alignment are quite high. Some of the misalignment effects can be compensated by rotating the whole reflector system in relation to the hologram, which eases the actual accuracy requirements. Nevertheless, the alignment of the reflectors is critical for satisfactory DRFS operation. To ensure sufficient accuracy the reflector system will be manufactured as an integrated system. The manufacturing and the mechanical design of the DRFS will be done by Thomas Keating Ltd in England.

Conclusions

The hologram based compact antenna test range can be improved with a dual reflector feed system. The relative quiet-zone size of the hologram CATR can be increased by modifying the hologram illumination with two shaped hyperbolic reflectors. The hologram manufacturing is facilitated when the modified illumination is used as very narrow slots are not needed at the hologram pattern edge. A simple geometrical optics based synthesis method was developed and implemented as an MATLAB[®]-software. The simulated hologram illumination agrees reasonably well with the desired illumination, which shows that the synthesis method is applicable to the dual reflector feed system design for the hologram CATR.

Acknowledgements

Individual authors are grateful to the Foundation for Commercial and Technical Sciences, the Foundation of Technology (Finland), the Foundation of the Finnish Society of Electronics Engineers, the Finnish Cultural Foundation, Jenny and Antti Wihuri Foundation and the Nokia Foundation for their support. This research is funded by ESA/ESTEC (ESTEC contract No.13096/98/NL/SB). VTT Information Technology is acknowledged for the use of GRASP8W software.

References

- [1] Foster, P. R., Martin, D., Parini, C., Räisänen, A., Ala-Laurinaho, J., Hirvonen, T., Lehto, A., Sehm, T., Tuovinen, J., Jensen, F., Pontoppidan, K., *Mmwave antenna testing techniques - Phase 2*, MAAS Report 304, Issue No. 2, ESTEC Contract No. 11641/95/NL/PB(SC), December 1996.
- [2] J. Ala-Laurinaho, T. Hirvonen, P. Piironen, A. Lehto, J. Tuovinen, A. V. Räisänen, U. Frisk, "Measurement of the Odin telescope at 119 GHz with a hologram type CATR", *IEEE Transactions on Antennas and Propagation*, Vol. 49, No. 9, pp. 1264–1270, 2001.
- [3] P.-S. Kildal, "Synthesis of multireflector antennas by kinematic and dynamic ray tracing", *IEEE Transactions on Antennas and Propagation*, Vol. 38, No. 10, pp. 1587–1599, 1990.